Monolithic multigrid for the marker-and-cell discretization of the Stokes–Darcy equations

Chen Greif, Yunhui He [ORCID] *

Department of Computer Science, The University of British Columbia, Vancouver, BC, Canada

A R T I C L E   I N F O

A B S T R A C T

We consider the marker-and-cell scheme for numerically solving the Stokes–Darcy equations. The corresponding discrete system has a double saddle-point structure. Designing a fast solver for such a problem is challenging o the different scales of the physical parameters. We propose a monolithic multigrid solver with a block-lower-triangular smoother based on the block-LU decomposition of the coefficient matrix, which requires solving a Poisson-type equation with a scalar Laplacian and two Schur complement systems. We demonstrate the robustness of a sparse approximate inverse smoother for the Laplacian, and we handle the Schur complement systems by applying simple relaxation schemes as smoothers. The proposed scheme is economical, and yet it is robust with respect to the mesh size and the physical parameters.

1. Introduction

We are interested in solving the discretized Stokes–Darcy equations, whose associated linear system has a double saddle-point structure. The coefficient matrix is typically large and sparse, and is often ill-conditioned. It may be nonsymmetric or symmetric indefinite, depending on the discretization and the boundary conditions. The challenge in developing an efficient numerical solver for such a linear system is due to the large scale of the problem and the different magnitudes of physical parameters. Our goal is to develop a fast iterative solution procedure.

Different types of discretizations have been developed and investigated for this problem: finite element methods [1–4], finite volume methods [5], and finite difference methods [6,7]. We will consider the marker-and-cell (MAC) finite difference scheme. A review of this method can be found in [8].

As far as iterative solvers are concerned, a number of preconditioners for Krylov subspace solvers for the mixed Stokes–Darcy model discretized by mixed finite elements have been proposed [9–12]. Recently, block-structured preconditioners for the MAC scheme were proposed and investigated [13], and incorporated into the GMRES iteration. They were shown to be effective for a large range of the physical parameters. However, their performance degrades when the physical parameter values are extremely small. In [9], the authors use a finite element formulation and apply a block diagonal preconditioner whose first two leading blocks are the discrete operators involved, and the third block is an approximation of the Schur complement. The inversion operation corresponds to solving two decoupled local problems. The authors of [11] partition the double saddle-point system into a 2-by-2 block system, and apply constraint preconditioning. In [12], the authors use a four-variable formulation, where a Lagrange multiplier is used, and apply operator preconditioning to derive a block diagonal preconditioner. The method is highly robust, but a fractional differential operator is used, which entails a high computational cost.

---

* Correspondence to: Department of Mathematics, University of Houston, Houston, TX, USA.
  E-mail address: yhe43@central.uh.edu (Y. He).

Multigrid methods form a formidable alternative to Krylov subspace solvers. The main challenge here is designing effective smoothers for the coupled discrete systems. A two-grid method is proposed in [14], which decouples the mixed model: a coarse-grid approximation is used for the interface conditions, and the fine-grid problem is decoupled into the Stokes and Darcy problems. In [15], the authors present a multigrid finite element method for the coupled problem, where one solves a small global problem on a coarse grid, and a series of Stokes and Darcy sub-problems on a fine grid. In [5], an Uzawa smoother is developed for the Stokes–Darcy problem discretized by finite volumes on staggered grids, where a decoupled procedure based on symmetric Gauss–Seidel smoothing is used for the velocity components and a simple Richardson iteration is used for the pressure field. The multigrid method considered in [5] is a domain-decomposition type algorithm, where multigrid is applied to two subdomains rather than the coupled system. The authors use local Fourier analysis (LFA) to analyze their proposed smoothers in each subdomain and demonstrate their effectiveness. In [10], the authors consider conforming and nonconforming finite element methods and finite volume methods for the coupled primal Stokes–Darcy problem. Three symmetric formulations are derived, and a block diagonal preconditioner based on norms in fractional Sobolev spaces is proposed, where, for each block, algebraic multigrid (AMG) solvers are used.

Our goal in this paper is to close an apparent gap in the design of monolithic multigrid methods for finite difference methods and offer a fast solver based on matrix–vector products. We design two block-lower-triangular smoothers based on the block-LU decomposition. One is based on a weighted Jacobi relaxation applied to the scalar Laplacian, and the other uses the sparse approximate inverse smoother for the scalar Laplacian proposed in [16]. For the first Schur complement that arises in our monolithic approach, we apply two sweeps of weighted Jacobi iterations as a smoother. The second Schur complement is nested, and here we use a Richardson scheme as a smoother. We remark that the presence of the interface conditions and the coupling violate the assumptions upon which LFA relies [17]. Therefore, we cannot perform an LFA analysis. In our numerical tests we adopt a trial-and-error approach for choosing the damping parameters. Our monolithic multigrid seems to be highly robust with respect to small physical parameters that [13] has some difficulty handling.

The remainder of this paper is organized as follows. In Section 2, we briefly present the MAC scheme for the Stokes–Darcy problem. In Section 3, we develop block-structured smoothers. In Section 4 numerical results are presented, demonstrating the robustness of our proposed multigrid method for the Stokes–Darcy problem with respect to meshsize and the physical parameters. Finally, we draw some conclusions in Section 5.

2. Discretization

Consider the coupled Stokes–Darcy problem in domain $\Omega = \Omega_d \bigcup \Omega_s$, see Fig. 1, where Γ is the interface of the two flow fluids. The Darcy equations in two dimensions are

$$\mathbb{K}^{-1}\boldsymbol{u}^d + \nabla p^d = 0, \quad \text{in } \Omega_d, \tag{1a}$$

$$\nabla \cdot \boldsymbol{u}^d = f^d, \quad \text{in } \Omega_d, \tag{1b}$$

where $\boldsymbol{u}^d = (u^d, v^d)$ is the velocity vector and p^d is the fluid pressure inside the porous medium. $\mathbb{K}$ is the hydraulic tensor, representing the properties of the porous medium and the fluid. Here we consider $\mathbb{K} = \kappa\mathbb{I}$, $\kappa > 0$, where $\mathbb{I}$ stands for an identity operator.

The free-flow problem is described by the Stokes equations

$$-\nu \triangle \boldsymbol{u}^s + \nabla p^s = \boldsymbol{f}^s, \quad \text{in } \Omega_s,$$

$$\nabla \cdot \boldsymbol{u}^s = 0, \quad \text{in } \Omega_s,$$

$$\boldsymbol{u}^s = g \quad \text{on } \partial\Omega_s,$$

where $\boldsymbol{u}^s = (u^s, v^s)$ is the fluid velocity vector, p^s is the scalar fluid pressure, and ν is the fluid viscosity.

Eqs. (1a)–(1b) can be rewritten as one equation

$$-\nabla \cdot (\kappa\nabla p^d) = f^d. \tag{2}$$

Then, the Stokes–Darcy problem can be written as a three-variables formulation for $(p^d, \boldsymbol{u}^s, p^s)$:

$$-\nabla \cdot (\kappa\nabla p^d) = f^d, \quad \text{in } \Omega_d, \tag{3a}$$

$$-\nu \triangle \boldsymbol{u}^s + \nabla p^s = \boldsymbol{f}^s, \quad \text{in } \Omega_s, \tag{3b}$$

$$\nabla \cdot \boldsymbol{u}^s = 0, \quad \text{in } \Omega_s, \tag{3c}$$

$$\boldsymbol{u}^s = g, \quad \text{on } \partial\Omega_s. \tag{3d}$$

To complete the model, we consider the following three interface conditions coupling the Stokes and the Darcy equations:

$$v^s = -\kappa\frac{\partial p^d}{\partial y}; \tag{4a}$$

$$p^s - p^d = 2\nu\frac{\partial v^s}{\partial y}; \tag{4b}$$

$$u^s = \frac{\nu}{\alpha}\left(\frac{\partial u^s}{\partial y} + \frac{\partial v^s}{\partial x}\right); \tag{4c}$$
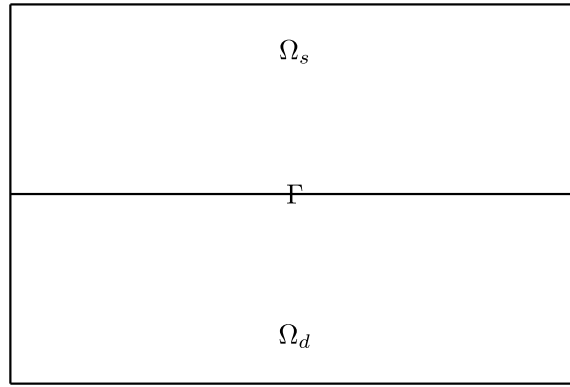
Fig. 1. A two-dimensional domain for the Stokes–Darcy problem. The interface is marked by Γ.

Eq. (4a) is a mass conservation condition, which guarantees continuity of normal velocity components. Eq. (4b) is a condition on the balance of normal forces, which allows the pressure to be discontinuous across the interface, and Eq. (4c) is the Beavers-Joseph-Saffman condition, providing a suitable slip condition on the tangential velocity. In the latter, the parameter α is experimentally determined and it depends on the properties of the porous medium.

2.1. Discretization

We follow [7] to present the well-known MAC scheme for the discretization of (3a), (3b), and (3c). Uniform staggered grids with meshsize $h = 1/n$ are used and the discrete values of (p^d, u^s, v^s, p^s) are placed at different locations; see Fig. 2. Specifically, the discrete values of p^d and p^s are placed at the cell centers and the discrete values of u^s and v^s are located at the grid cell faces. Stability and convergence analysis of the MAC scheme considered here can be found in [7]. For the Laplace operator, we consider the standard five-point finite different discretization, whose stencil notation is given by

$$-\Delta_h = \frac{1}{h^2}\begin{bmatrix} & -1 & \\ -1 & 4 & -1 \\ & -1 & \end{bmatrix}.$$

For the gradient operator, we consider a second-order approximation,

$$(\partial_x)_{h/2} = \frac{1}{h}\begin{bmatrix} -1 & 0 & 1 \end{bmatrix}, \quad (\partial_y)_{h/2} = \frac{1}{h}\begin{bmatrix} -1 \\ 0 \\ 1 \end{bmatrix},$$

where 0 is the location of the meshpoint where the discretization is applied.

For details on the discretization of the three interface conditions (4), we refer the reader to [7,13]. Incorporating the discretization of the boundary conditions and symmetrizing the off-diagonal blocks [13], the discrete Stokes–Darcy equations lead to a saddle point structure system

$$\mathcal{L}_h z_h = \begin{pmatrix} \mathcal{A} & \mathcal{B}^T \\ \mathcal{B} & 0 \end{pmatrix}\begin{pmatrix} \boldsymbol{x} \\ \boldsymbol{y} \end{pmatrix} = \begin{pmatrix} b_1 \\ b_2 \end{pmatrix} = b_h, \tag{5}$$

where

$$\mathcal{A} = \begin{pmatrix} A_1 & G^T \\ G & -A_2 \end{pmatrix}, \quad \mathcal{B} = \begin{pmatrix} 0 & B \end{pmatrix}.$$

Here, A_1 corresponds to $-\kappa \Delta p^d$, which is symmetric. The operator A_2 stands for $-\nu \Delta u^s$ and the discretization of the interface variables v^s. Due to the interface conditions (4a)–(4c), the matrix A_2 is nonsymmetric, see details in [13]. $\boldsymbol{x}$ is the vector of the discrete values of p^d and $-u^s$, and $\boldsymbol{y}$ is the vector of the discrete values of p^s. G^T has a simple structure given by [13]

$$G^T = \begin{pmatrix} 0 & 0 & 0 \\ 0 & -I_n/h & 0 \end{pmatrix},$$
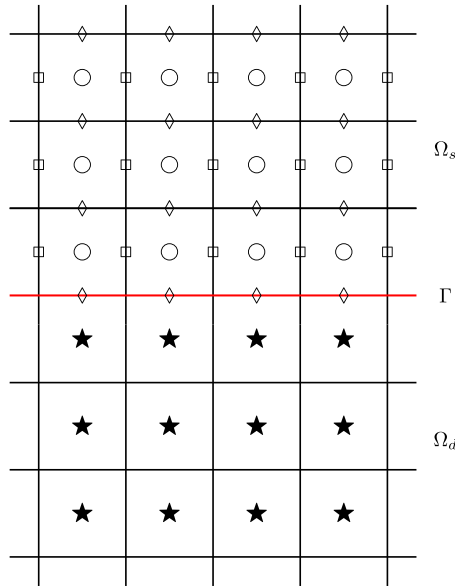
where I_n is an identity matrix of dimension n.

Fig. 2. The locations of the unknowns on staggered grids. The variables: $\square - u^s$, $\Diamond - v^s$, $\bigcirc - p^s$, and $\bigstar - p^d$.

Algorithm 1 A two-grid method: $z_h^{j+1} = \textbf{TwoGrid}(\mathcal{L}_h, b_h, z_h^j, \eta_1, \eta_2)$

1: Pre-smoothing: Applying η_1 sweeps of relaxation to z_h^j:

$$\bar{z}_h^j = \textbf{Smoothing}(\mathcal{L}_h, b_h, z_h^j, \eta_1).$$

2: Coarse–grid correction procedure:

- Compute the residual: $r_h = b_h - \mathcal{L}_h \bar{z}_h^j$;
- Restrict the residual: $r_H = \mathcal{R}_h r_h$;
- Solve the coarse-grid problem: $\mathcal{L}_H u_H = r_H$;
- Interpolate the correction: $\delta z_h = \mathcal{P}_h z_H$;
- Update the corrected approximation: $\hat{z}_h^j = \bar{z}_h^j + \delta z_h$;

3: Post-smoothing: Applying η_2 sweeps of relaxation to $\hat{z}_h^j$,

$$z_h^{j+1} = \textbf{Smoothing}(\mathcal{L}_h, b_h, \hat{z}_h^j, \eta_2)$$

---

3. Monolithic multigrid

The basic idea of the multigrid method is to iteratively solve a series of small-dimension linear systems defined on mesh grids Ω_{h_i}. There are two stages: relaxation or smoothing and coarse-grid correction (CGC). Given a current approximation z_h^j, we update this approximation via

$$z_h^j \leftarrow z_h^j + \omega \mathcal{M}_h^{-1}(b_h - \mathcal{L}_h z_h^j), \tag{6}$$

where $\mathcal{M}_h$ is a smoother, capable of reducing the high frequencies residual error, and ω is a damping parameter to be determined. In this process, often a few iterations are enough, and then we restrict the new residual onto a coarser grid, where we can solve a small linear system. We give a two-grid method diagram in Algorithm 1. In the CGC, one can solve the coarse-grid problem $\mathcal{L}_H u_H = r_H$ iteratively. Doing so, we obtain a multigrid scheme. $\mathcal{R}_h$ and $\mathcal{P}_h$ are grid-transfer operators.

In general, a two-grid error operator is given by

$$E = S_h^{\eta_2}(I - \mathcal{P}_h \mathcal{L}_H^{-1} \mathcal{R}_h \mathcal{L}_h) S_h^{\eta_1}, \tag{7}$$

where $S_h = I - \omega \mathcal{M}_h^{-1} \mathcal{L}_h$, and η_1 and η_2 are the number of pre- and postsmoothing steps. In the sequel, for simplicity, we omit the subscript h unless it is necessary.

3.1. Smoothers

It has been numerically shown [13] that the eigenvalue distribution of $\mathcal{L}$ highly depends on the physical parameters, ν and κ, and might have complex or negative eigenvalues. In [13], we consider the following operator as a preconditioner for the Stokes–Darcy system,

$$
P = \begin{pmatrix} A_1 & 0 & 0 \\ G & -S_1 & 0 \\ 0 & B & S_2 \end{pmatrix}, \tag{8}
$$

where the two Schur complements are given by

$$
S_1 = A_2 + G A_1^{-1} G^T \quad \text{and} \quad S_2 = B S_1^{-1} B^T.
$$

For this choice, the eigenvalues of $P^{-1}\mathcal{L}$ are all ones. However, solving the Schur complement systems with S_1 and S_2 exactly is computationally costly. In practice, one has to find approximate solutions for these systems; see [13] for more discussion.

Motivated by the block lower-triangular structure of P, we consider a smoother for $\mathcal{L}$ in the form

$$
\mathcal{M} = \begin{pmatrix} W_0 & 0 & 0 \\ G & -W_1 & 0 \\ 0 & B & W_2 \end{pmatrix}, \tag{9}
$$

where W_0 has strong smoothing property on A_1, and

$$
W_1 = A_2 + G W_0^{-1} G^T \quad \text{and} \quad W_2 = \frac{1}{\nu} I, \tag{10}
$$

where I stands for an identity matrix.

In (6), we solve the following system

$$
\mathcal{M} \begin{pmatrix} d_1 \\ d_2 \\ d_3 \end{pmatrix} = \begin{pmatrix} r_1 \\ r_2 \\ r_3 \end{pmatrix}. \tag{11}
$$

Using (9), the solution of (11) can be updated via the three steps:

$$
W_0 d_1 = r_1, \tag{12a}
$$

$$
W_1 d_2 = -r_2 + G d_1, \tag{12b}
$$

$$
d_3 = \nu(r_3 - B d_2). \tag{12c}
$$

Next, we discuss how to approximate the linear operators of systems (12a) and (12b).

Solving system (12a). Recall that A_1 corresponds to the discretization of $-\kappa \Delta p^d$ on cell centers, which is just a scaled negative Laplacian. In the literature, there are many fast multigrid solvers for such systems, where only matrix–vector products are needed.

One simple choice is weighted Jacobi,

$$
W_{0,J}^{-1} = \frac{4}{5} \mathrm{diag}(A_1)^{-1}. \tag{13}
$$

We also consider a sparse approximate inverse smoother proposed in [16], whose stencil is given by

$$
M_S = \frac{h^2}{24} \begin{bmatrix} 3 & 10 & 3 \\ 10 & 44 & 10 \\ 3 & 10 & 3 \end{bmatrix}. \tag{14}
$$

This smoother leads to an optimal smoothing convergence factor of 0.1595 with the optimal damping parameter $\omega = 0.1576$ for the Poisson problem with a Laplacian discretized using the five-point standard stencil. Thus, we consider another stencil choice of W_0 given by

$$
W_{0,S}^{-1} = \frac{0.1576}{\kappa} \cdot \frac{h^2}{24} \begin{bmatrix} 3 & 10 & 3 \\ 10 & 44 & 10 \\ 3 & 10 & 3 \end{bmatrix}. \tag{15}
$$

With those choices, the solution d_1 in (12a) is approximated by the matrix–vector product

$$
d_1 = W_{0,*}^{-1} r_1, \tag{16}
$$

where $*$ stands for either of the options we are considering, J or S. Here, we use the same notation for the stencil and its corresponding assembled matrix.

Solving the Schur complement system (12b). Since we know the explicit form of the inverse of W_0, and G is a sparse matrix with only one nonzero small block, which is a scaled identity, the matrix $W_1 = A_2 + G W_0^{-1} G^T$ can be easily formed. Solving (12b) exactly

is expensive, so we consider two sweeps of weighted Jacobi iterations on (12b).

We choose $W_0 = W_{0,J}$ and $W_0 = W_{0,S}$, and denote the corresponding preconditioner $\mathcal{M}$ in (9) as $\mathcal{M}_J$ and $\mathcal{M}_S$, respectively. Furthermore, when using two sweeps of the weighted Jacobi solve for W_1, we denote the corresponding inexact versions of $\mathcal{M}$ as $\mathcal{M}_{J,I}$ and $\mathcal{M}_{S,I}$, respectively. Using these approximations, the solution of (11) can be computed by matrix–vector products and inversion of diagonal matrices.

3.2. Grid-transfer operators

We now introduce the grid-transfer operators for the velocity and pressure unknowns [18]. For the velocity vector, 6-point stencils are often used given by the stencils

$$R_{u^s} = \frac{1}{8}\begin{bmatrix} 1 & 2 & 1 \\ & \bullet & \\ 1 & 2 & 1 \end{bmatrix}, \quad R_{v^s} = \frac{1}{8}\begin{bmatrix} 1 & & 1 \\ 2 & \bullet & 2 \\ 1 & & 1 \end{bmatrix}, \tag{17}$$

for u^s and v^s, respectively. The notation $\bullet$ marks where the operator is applied at.

For the Stokes pressure p^s and the Darcy variable p^d, a four-point stencil is used, that is,

$$R_{p^s} = R_{p^d} = \frac{1}{4}\begin{bmatrix} 1 & & 1 \\ & \bullet & \\ 1 & & 1 \end{bmatrix}. \tag{18}$$

Thus, for the coupled system, we consider the restriction operator

$$\mathcal{R} = \begin{bmatrix} R_\phi & 0 & 0 & 0 \\ 0 & R_u & 0 & 0 \\ 0 & 0 & R_v & 0 \\ 0 & 0 & 0 & R_p \end{bmatrix}. \tag{19}$$

We take $\mathcal{P} = 4\mathcal{R}^T$.

4. Numerical results

In this section, we consider an example presented in [5] to demonstrate the performance of the proposed multigrid scheme. Let $\Omega_s = [0,1] \times [0,1]$ and $\Omega_d = [0,1] \times [-1,0]$. The equation is constructed so that the analytical solution is given by

$$u^s = \lambda'(y)\cos x,$$
$$v^s = \lambda(y)\sin x,$$
$$p^s = 0,$$
$$p^d = e^y \sin x,$$

where

$$\lambda(y) = -\kappa - \frac{y}{2\nu} + \left(-\frac{\alpha}{4\nu^2} + \frac{\kappa}{2}\right)y^2.$$

In our numerical tests, we choose $\alpha = \nu$. We are interested to explore how our methods are affected by the physical parameters ν, κ and the meshsize h.

4.1. Eigenvalue distribution

We first look at the eigenvalues of $\mathcal{M}^{-1}\mathcal{L}$ with the two choices of $\mathcal{M}$ discussed in Section 3.1. Here, we fix $n = 32$ and consider two pairs of physical parameters: $(\nu, \kappa) = (1, 1)$ and $(\nu, \kappa) = (1, 10^{-8})$.

From Fig. 3, we see that for $\nu = 1$ and $\kappa = 1$, the eigenvalues of $\mathcal{M}_J^{-1}\mathcal{L}$ are complex, but their imaginary parts have very small magnitudes across the board. The real parts of all eigenvalues are positive, which is a desirable property for multigrid convergence. For $\nu = 1$ and $\kappa = 10^{-8}$, the eigenvalues of matrix $\mathcal{M}_J^{-1}\mathcal{L}$ have a large imaginary magnitude compared with the case of $(\nu, \kappa) = (1, 1)$. This might explain why multigrid takes more iterations to solve the discrete Stokes–Darcy problem with small value of κ, see Section 4.2.1.

Fig. 4 shows the eigenvalues of $\mathcal{M}_S^{-1}\mathcal{L}$ with $(\nu, \kappa) = (1, 1)$ and $(\nu, \kappa) = (1, 10^{-8})$. When $\nu = \kappa = 1$, the eigenvalue distribution of $\mathcal{M}_S^{-1}\mathcal{L}$ seems similar to that of $\mathcal{M}_J^{-1}\mathcal{L}$. For $\nu = 1$ and $\kappa = 10^{-8}$, on the other hand, the eigenvalues of $\mathcal{M}_S^{-1}\mathcal{L}$ seem to be slightly more clustered compared to those of $\mathcal{M}_J^{-1}\mathcal{L}$. This might explain why $\mathcal{M}_S^{-1}\mathcal{L}$ performs better than $\mathcal{M}_J^{-1}\mathcal{L}$ discussed in Section 4.2.

The eigenvalue distribution of $\mathcal{M}^{-1}\mathcal{L}$ might suggest that for small values of κ, the discrete system is hard to solve due to the large imaginary parts of the complex eigenvalues.
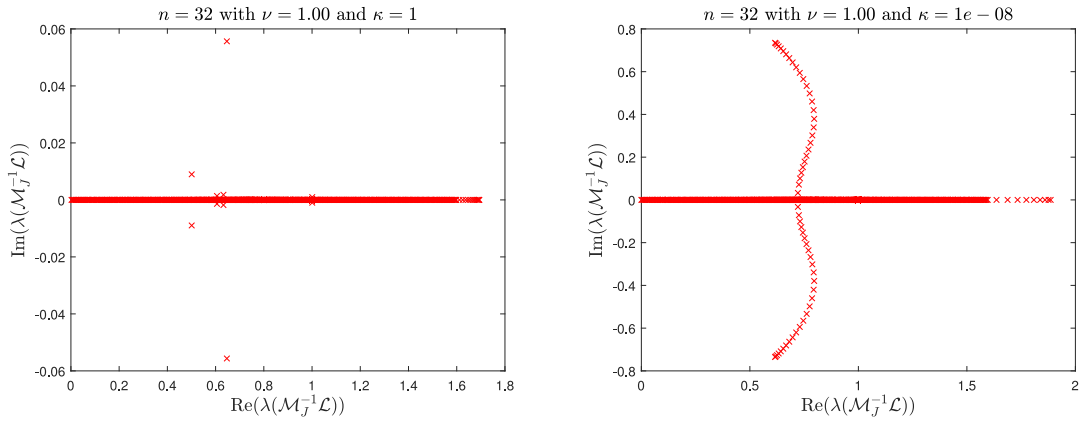
Fig. 3. The eigenvalue distribution of $\mathcal{M}_J^{-1}\mathcal{L}$ for $(\nu, \kappa) = (1, 1)$ and $(\nu, \kappa) = (1, 10^{-8})$ with $n = 32$.
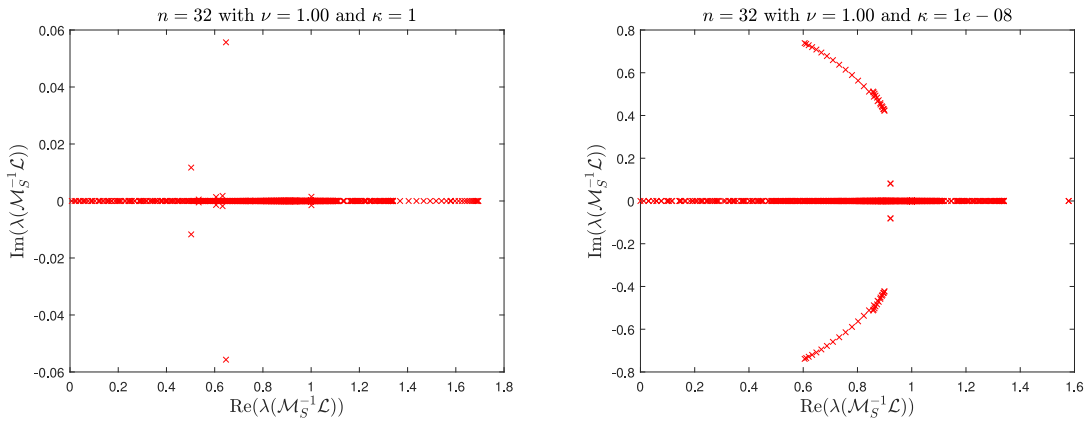

Fig. 4. The eigenvalue distribution of $\mathcal{M}_S^{-1}\mathcal{L}$ for $(\nu, \kappa) = (1, 1)$ and $(\nu, \kappa) = (1, 10^{-8})$ with $n = 32$.

4.2. Multigrid performance

We now report results related to the performance of the proposed multigrid scheme. We use a uniform mesh with the finest meshsize denoted by h. Let $d_h^j = b_h - \mathcal{L}_h z_h^j$, where z_h^j is the approximation to the solution of (5) at the jth multigrid iteration. We report the number of iterations j taken to satisfy the stopping criterion $\|d_h^j\|_\infty / \|d_h^0\|_\infty < 10^{-8}$. The initial guess z_h^0 is chosen randomly. The setup of our tests is as follows.

- When applying two sweeps of weighted Jacobi iterations with weight 0.8 for W_1, we use a zero initial guess.
- The operator is re-discretized on coarser meshes.
- The coarsest grids for Ω_d and Ω_s are both 4×4.
- We take $\eta_1 = \eta_2 = 3$; see Algorithm 1 for the two-grid method.

We first report the iteration counts using different smoothing steps in Table 1 to explain why we choose $\eta_1 = \eta_2 = 3$ in our subsequent tests. We observe that increasing the smoothing steps decreases the iteration numbers, but there is no significant change for $\eta_1 = \eta_2 > 3$.

4.2.1. Jacobi-based smoother

In the smoothing process, there is a damping parameter ω in (6) to be determined. We experimentally find that $\omega = 0.9$ yields a good performance for a large range of values of ν, κ, especially for small values. Thus we take this value for all Jacobi-based smoother multigrid tests.

In we show the two-grid performance using smoother $\mathcal{M}_J$ for fixed $h = 1/64$ and varying $\nu = \kappa$, where we solve the system of W_1 exactly. It is evident from that the solver shows a rather satisfactory level of robustness and scalability with respect to ν and κ.

As a practical solver, we consider an inexact solve for W_1. We have tried one sweep iteration of weighted Jacobi, and found that it takes more than 50 two-grid iterations to reach the stopping criterion, but using two sweeps of Jacobi iterations significantly

Table 1
W-cycle iteration counts for different smoothers and different numbers of smoothing steps with fixed $h = 1/128$ and $v = 1$. We take $\omega = 0.9$ and 1 in (6) for $\mathcal{M}_{J,I}$ and $\mathcal{M}_{S,I}$, respectively. The symbol '–' stands for divergence of Algorithm 1 and κ is the parenthetical value associated to the smoother in the top row of the table.

(η_1, η_2)	$\mathcal{M}_{J,I}(1)$	$\mathcal{M}_{J,I}(10^{-8})$	$\mathcal{M}_{S,I}(1)$	$\mathcal{M}_{S,I}(10^{-8})$
$(1,1)$	18	–	16	45
$(2,2)$	11	54	8	21
$(3,3)$	8	20	7	11
$(4,4)$	7	16	6	12

Table 2
Two-grid iteration counts using $\mathcal{M}_J$ for the coupled Stokes–Darcy problem varying κ and v with fixed $h = 1/64$.

κ \ v	10^0	10^{-1}	10^{-2}	10^{-3}	10^{-4}	10^{-5}	10^{-6}	10^{-7}	10^{-8}
10^0	8	7	6	8	11	13	15	17	18
10^{-1}	8	8	9	9	11	13	15	17	19
10^{-2}	8	11	12	9	11	13	15	17	19
10^{-3}	11	12	10	7	10	12	13	15	17
10^{-4}	12	10	8	6	8	10	12	14	15

Table 3
Two-grid iteration counts using $\mathcal{M}_{J,I}$ for the coupled Stokes–Darcy problem varying κ and v with fixed $h = 1/64$.

κ \ v	10^0	10^{-1}	10^{-2}	10^{-3}	10^{-4}	10^{-5}	10^{-6}	10^{-7}	10^{-8}
10^0	8	7	7	7	11	14	15	17	19
10^{-1}	8	7	6	9	12	13	15	17	19
10^{-2}	8	7	8	10	11	13	15	17	19
10^{-3}	8	9	10	8	10	12	14	16	17
10^{-4}	9	10	8	7	8	10	12	14	16

Table 4
W-cycle multigrid iteration counts using $\mathcal{M}_{J,I}$ for the coupled Stokes–Darcy problem varying $h = 1/n$ and κ with fixed $v = 1$.

κ \ n	10^0	10^{-1}	10^{-2}	10^{-3}	10^{-4}	10^{-5}	10^{-6}	10^{-7}	10^{-8}
32	8	7	7	11	15	14	17	19	21
64	8	7	7	7	13	15	16	18	20
128	8	7	7	7	9	15	13	17	20
256	8	7	7	7	7	12	15	16	18
512	8	7	7	7	7	8	14	14	17

Table 5
W-cycle multigrid iteration counts using $\mathcal{M}_{J,I}$ for the coupled Stokes–Darcy problem varying κ and v with fixed $h = 1/128$.

κ \ v	10^0	10^{-1}	10^{-2}	10^{-3}	10^{-4}	10^{-5}	10^{-6}	10^{-7}	10^{-8}
10^0	8	7	7	7	9	15	13	17	19
10^{-1}	8	7	7	8	13	11	15	18	20
10^{-2}	8	7	7	10	10	13	15	18	20
10^{-3}	8	8	11	10	10	12	14	17	19
10^{-4}	8	11	10	8	8	10	12	14	17

accelerates convergence. Thus, in the following, we take two Jacobi sweeps for all tests. shows the two-grid performance using the inexact Jacobi-based smoother $\mathcal{M}_{J,I}$. We see the iteration counts in are almost the same as these for the exact solution for the smoother in .

Next, we examine W-cycle performance for the inexact version. reports W-cycle performance with fixed $v = 1$ and varying h and κ. We can see in each column of table that , the multigrid performance is h-independent. In each row (fixing n), we see the iteration number increasing with decreasing κ. In , we fix $h = 1/128$ and vary v and κ, using a W-cycle. We observe that the solver has difficulties keeping the iteration counts constant for small values of κ. This illustrates the challenging nature of this problem.

Finally, we present F-cycle results in . We see that the F-cycle has similar performance to that of W-cycle shown in , except for $\kappa = 10^{-6}, 10^{-7}, 10^{-8}$, where the F-cycle takes one or two more iterations, compared with W-cycle.

Table 6
F-cycle multigrid iteration counts using $\mathcal{M}_{J,I}$ for the coupled Stokes–Darcy problem varying κ and ν with fixed $h = 1/128$.

ν \ κ	10^0	10^{-1}	10^{-2}	10^{-3}	10^{-4}	10^{-5}	10^{-6}	10^{-7}	10^{-8}
10^0	8	7	7	7	11	15	14	18	21
10^{-1}	8	7	6	9	13	11	16	19	21
10^{-2}	8	7	8	11	10	14	16	19	21
10^{-3}	8	10	11	10	10	13	15	18	20
10^{-4}	10	11	10	8	8	11	13	15	18

Table 7
Two-grid iteration counts using $\mathcal{M}_S$ for the coupled Stokes–Darcy problem varying κ and ν with fixed $h = 1/64$.

ν \ κ	10^0	10^{-1}	10^{-2}	10^{-3}	10^{-4}	10^{-5}	10^{-6}	10^{-7}	10^{-8}
10^0	7	7	7	7	8	8	9	10	10
10^{-1}	6	7	7	7	7	8	9	10	11
10^{-2}	6	7	7	6	7	8	9	10	11
10^{-3}	8	7	5	5	6	8	8	9	10
10^{-4}	7	5	5	5	5	6	7	8	9

Table 8
Two-grid iteration counts using $\mathcal{M}_{S,I}$ for the coupled Stokes–Darcy problem varying κ and ν with fixed $h = 1/64$.

ν \ κ	10^0	10^{-1}	10^{-2}	10^{-3}	10^{-4}	10^{-5}	10^{-6}	10^{-7}	10^{-8}
10^0	7	7	7	6	8	8	9	10	11
10^{-1}	6	6	6	7	7	8	9	10	11
10^{-2}	6	6	6	6	7	8	9	10	11
10^{-3}	7	7	7	7	7	7	8	9	10
10^{-4}	7	7	7	7	7	7	7	8	9

Table 9
W-cycle multigrid iteration counts using $\mathcal{M}_{S,I}$ for the coupled Stokes–Darcy problem varying $h = 1/n$ an κ with fixed $\nu = 1$.

n \ κ	10^0	10^{-1}	10^{-2}	10^{-3}	10^{-4}	10^{-5}	10^{-6}	10^{-7}	10^{-8}
32	7	7	7	8	8	8	10	10	12
64	7	7	7	7	9	8	9	10	11
128	7	7	7	7	7	9	9	10	11
256	7	7	7	7	7	8	8	9	10
512	7	7	7	7	7	7	9	9	10

4.2.2. Sparse approximate inverse based-smoother

We now demonstrate the robustness of a sparse approximate inverse for the Laplacian-based smoother with respect to the physical parameters. We find that taking $\omega = 1$ or $\omega = 0.9$ in (6) gives almost the same iteration counts (one or two iterations difference in some cases). Thus, for simplicity, we choose $\omega = 1$ in our tests.

In , we show the two-grid multigrid performance using the sparse approximate inverse smoother $\mathcal{M}_S$, where we solve the W_1 system exactly. In we show the performance of the inexact smoother $\mathcal{M}_{S,J}$, where two sweeps of weighted Jacobi iterations are applied to the Schur complement system with W_1. We observe that $\mathcal{M}_{S,I}$ has a similar performance, compared to $\mathcal{M}_S$. Comparing with , we conclude that for large values of κ, the Jacobi-based smoother and sparse approximate inverse smoother perform similarly, but for small values of κ, the performance of $\mathcal{M}_{S,I}$ is much better than that of $\mathcal{M}_{J,I}$. Since the computational cost of the approximate inverse solver is rather modest, our overall conclusion is that this solver is more robust for the challenging range of small physical parameters.

shows W-cycle performance of $\mathcal{M}_{S,J}$ for a fixed $\nu = 1$ and varying h and κ. We see similar results of two-grid performance. shows W-cycle performance of $\mathcal{M}_{S,J}$ for fixed $h = 1/128$ and varying ν and κ. Again, the performance is similar to that of two-grid method. In , we present the F-cycle performance for fixed $h = 1/128$ by varying ν and κ, where we see a similar performance to that of W-cycle.

Finally, we comment that degradation is observed for the V-cycle multigrid scheme, especially for small values of κ. Thus, we recommend using the W-cycle scheme.

Table 10

W-cycle multigrid iteration counts using $\mathcal{M}_{S,I}$ for the coupled Stokes–Darcy problem varying κ and ν with fixed $h = 1/128$.

ν \ κ	10^0	10^{-1}	10^{-2}	10^{-3}	10^{-4}	10^{-5}	10^{-6}	10^{-7}	10^{-8}
10^0	7	7	7	7	7	9	9	10	11
10^{-1}	6	6	6	7	8	8	9	10	11
10^{-2}	6	6	6	6	7	8	9	10	11
10^{-3}	7	7	7	7	7	7	8	9	10
10^{-4}	7	7	7	7	7	7	7	8	9

Table 11

F-cycle multigrid iteration counts using $\mathcal{M}_{S,I}$ for the coupled Stokes–Darcy problem varying κ and ν with fixed $h = 1/128$.

ν \ κ	10^0	10^{-1}	10^{-2}	10^{-3}	10^{-4}	10^{-5}	10^{-6}	10^{-7}	10^{-8}
10^0	7	7	7	7	8	9	9	10	11
10^{-1}	6	6	6	7	8	8	9	10	11
10^{-2}	6	6	6	6	7	8	9	10	11
10^{-3}	7	7	7	7	7	7	8	9	10
10^{-4}	7	7	7	7	7	7	7	8	9

5. Conclusion

We have proposed two block lower-triangular smoothers for the MAC-discretized Stokes–Darcy equations. Two smoothers for the scalar Laplacian have been considered. One is based on Jacobi and the other is a sparse approximate inverse. We have observed that the latter is more robust for small values of the physical parameters, and we recommend using it as the method of choice. During the smoothing process, we also need to deal with two Schur complement systems. We apply two sweeps of weighted Jacobi iterations for the first system, and a Richardson scheme for the second.

Our multigrid scheme only requires matrix–vector products and the action of inverting diagonal matrices. The sparse approximate inverse, used in conjunction with W-cycle multigrid, shows promise in terms of robustness and scalability for a large range of values of the meshsize h and the physical parameters.

We have limited ourselves to uniform meshes and a specific set of values of the damping parameter ω. Developing fast multigrid methods for non-uniform grids and more challenging computational domains is a potentially useful goal for future work. Another useful goal is to consider heterogeneous anisotropic media.

Acknowledgments

Data availability

No data was used for the research described in the article.

References

[1] T. Karper, K.-A. Mardal, R. Winther, Unified finite element discretizations of coupled Darcy–Stokes flow, Numer. Methods Partial Differential Equations 25 (2) (2009) 311–326.

[2] K.A. Mardal, X.-C. Tai, R. Winther, A robust finite element method for Darcy–Stokes flow, SIAM J. Numer. Anal. 40 (5) (2002) 1605–1631.

[3] S. Zhang, X. Xie, Y. Chen, Low order nonconforming rectangular finite element methods for Darcy-Stokes problems, J. Comput. Math. (2009) 400–424.

[4] W. Chen, F. Wang, Y. Wang, Weak Galerkin method for the coupled Darcy–Stokes flow, IMA J. Numer. Anal. 36 (2) (2016) 897–921.

[5] P. Luo, C. Rodrigo, F.J. Gaspar, C.W. Oosterlee, Uzawa smoother in multigrid for the coupled porous medium and Stokes flow system, SIAM J. Sci. Comput. 39 (5) (2017) S633–S661.

[6] H. Rui, Y. Sun, A MAC scheme for coupled Stokes–Darcy equations on non-uniform grids, J. Sci. Comput. 82 (3) (2020) 1–29.

[7] M.-C. Shiue, K.C. Ong, M.-C. Lai, Convergence of the MAC scheme for the Stokes/Darcy coupling problem, J. Sci. Comput. 76 (2) (2018) 1216–1251.

[8] S. McKee, M.F. Tomé, V.G. Ferreira, J.A. Cuminato, A. Castelo, F. Sousa, N. Mangiavacchi, The MAC method, Comput. & Fluids 37 (8) (2008) 907–930.

[9] M. Cai, M. Mu, J. Xu, Preconditioning techniques for a mixed Stokes/Darcy model in porous media applications, J. Comput. Appl. Math. 233 (2) (2009) 346–355.

[10] W.M. Boon, T. Koch, M. Kuchta, K.-A. Mardal, Robust monolithic solvers for the Stokes–Darcy problem with the Darcy equation in primal form, SIAM J. Sci. Comput. 44 (4) (2022) B1148–B1174.

[11] P. Chidyagwai, S. Ladenheim, D.B. Szyld, Constraint preconditioning for the coupled Stokes–Darcy system, SIAM J. Sci. Comput. 38 (2) (2016) A668–A690.

[12] K.E. Holter, M. Kuchta, K.-A. Mardal, Robust preconditioning for coupled Stokes–Darcy problems with the Darcy problem in primal form, Comput. Math. Appl. 91 (2021) 53–66.

[13] C. Greif, Y. He, Block preconditioners for the Marker and Cell discretization of the Stokes–Darcy equations, SIAM J. Matrix Anal. Appl. 44 (4) (2023) 1540–1565.

[14] M. Mu, J. Xu, A two-grid method of a mixed Stokes–Darcy model for coupling fluid flow with porous media flow, SIAM J. Numer. Anal. 45 (5) (2007) 1801–1813.

[15] L. Zuo, G. Du, A multi-grid technique for coupling fluid flow with porous media flow, Comput. Math. Appl. 75 (11) (2018) 4012–4021.

[16] Y. He, J. Liu, X.-S. Wang, Optimized sparse approximate inverse smoothers for solving Laplacian linear systems, Linear Algebra Appl. 656 (2023) 304–323.

[17] U. Trottenberg, C.W. Oosterlee, A. Schuller, Multigrid, Elsevier, 2000.

[18] A. Niestegge, K. Witsch, Analysis of a multigrid Stokes solver, Appl. Math. Comput. 35 (3) (1990) 291–303.